



1       **THE MUMBA CAMPAIGN: MEASUREMENTS OF**  
2                   **URBAN, MARINE AND BIOGENIC AIR**

3

4       **Clare Paton-Walsh<sup>1\*</sup>, Élise-Andrée Guérette<sup>1</sup>, Dagmar Kubistin<sup>1</sup>, Ruhi Humphries<sup>1,2</sup>,**  
5       **Stephen R. Wilson<sup>1</sup>, Doreena Dominick<sup>1</sup>, Ian Galbally<sup>1,2</sup>, Rebecca Buchholz<sup>1,3</sup>,**  
6       **Mahendra Bhujel<sup>1,2</sup>, Scott Chambers<sup>4</sup>, Min Cheng<sup>2</sup>, Martin Cope<sup>2</sup>, Perry Davy<sup>5</sup>,**  
7       **Kathryn Emmerson<sup>2</sup>, David W. T. Griffith<sup>1</sup>, Alan Griffiths<sup>4</sup>, Melita Keywood<sup>2</sup>,**  
8       **Sarah Lawson<sup>2</sup>, Suzie Molloy<sup>2</sup>, Géraldine Rea<sup>1,6</sup>, Paul Selleck<sup>2</sup>, Xue Shi<sup>1</sup>, Jack**  
9       **Simmons<sup>1</sup> and Voltaire Velazco<sup>1</sup>**

10

11       <sup>1</sup> Centre for Atmospheric Chemistry, School of Chemistry, University of Wollongong,  
12       Northfields Avenue, Wollongong, N.S.W. Australia.

13       <sup>2</sup> CSIRO Climate Science Centre, Aspendale, Victoria, Australia.

14       <sup>3</sup> Atmospheric Chemistry Observations & Modeling (ACOM) Laboratory, National Center for  
15       Atmospheric Research, Boulder, CO, USA

16       <sup>4</sup> ANSTO, Environmental Research, Locked Bag 2001, Kirrawee DC, NSW 2232, Australia.

17       <sup>5</sup> GNS Science, National Isotope Centre, Lower Hutt, NZ.

18       <sup>6</sup> Université Pierre et Marie Curie, Laboratoire de Météorologie Dynamique - CNRS/IPSL  
19       Ecole Polytechnique 91128 Palaiseau Cedex, Paris, France.

20

21       \* Author to whom correspondence should be addressed; Clare Paton-Walsh (Murphy)  
22       (E-Mail: clarem@uow.edu.au); Tel.: +61-2-4221-5065; Fax: +61-2-4221-4287;

23

24



1 **Abstract**

2 The Measurements of Urban, Marine and Biogenic Air (MUMBA) campaign took place in  
3 Wollongong, New South Wales (a small coastal city approximately 80 km south of Sydney,  
4 Australia), from 21<sup>st</sup> December 2012 to 15<sup>th</sup> February 2013. Like many Australian cities,  
5 Wollongong is surrounded by dense eucalyptus forest and so the urban air-shed is heavily  
6 influenced by biogenic emissions. Instruments were deployed during MUMBA to measure  
7 the gaseous and aerosol composition of the atmosphere with the aim of providing a detailed  
8 characterisation of the complex environment of the ocean/forest/urban interface that could be  
9 used to test the skill of atmospheric models. Gases measured included ozone, oxides of  
10 nitrogen, carbon monoxide, carbon dioxide, methane and many of the most abundant volatile  
11 organic compounds. Aerosol characterisation included total particle counts above 3 nm, total  
12 cloud condensation nuclei counts; mass concentration, number concentration size  
13 distribution, aerosol chemical analyses and elemental analysis.

14 The campaign captured varied meteorological conditions, including two extreme heat events,  
15 providing a potentially valuable test for models of future air quality in a warmer climate.  
16 There was also an episode when the site sampled clean marine air for many hours, providing  
17 a useful additional measure of background concentrations of these trace gases within this  
18 poorly sampled region of the globe. In this paper we describe the campaign, the meteorology  
19 and the resulting observations of atmospheric composition in general terms, in order to equip  
20 the reader with sufficient understanding of the Wollongong regional influences to use the  
21 MUMBA datasets as a case study for testing a chemical transport model. The data is  
22 available from PANGAEA (see <http://doi.pangaea.de/10.1594/PANGAEA.871982>).

23

24

25 **Keywords:** VOCs, Ozone, Greenhouse Gases, Aerosols, Air Quality, Measurement  
26 Campaign,

27

28 **1. Introduction**

29 The value of intensive measurement campaigns in helping to understand and characterise  
30 local atmospheric composition and air quality has been recognised from as early as 1969,  
31 when the Los Angeles Smog Project took place [Whitby *et al.*, 1972b]. Since then, many such  
32 campaigns have focused on understanding the formation of photochemical smog in the most



1 polluted cities worldwide, with early efforts concentrated in the USA, (e.g. in [Gray *et al.*,  
2 1986; Husar *et al.*, 1972; Whitby *et al.*, 1972a]). The formation of secondary organic aerosol  
3 has also been of particular interest, with many studies using elemental carbon (black carbon)  
4 as an indicator of primary emissions; when the ratio of organic carbon to elemental carbon in  
5 the sampled air is higher than expected from the ratio of the primary emissions, secondary  
6 organic aerosol formation is indicated [Castro *et al.*, 1999; Gray *et al.*, 1986; Turpin and  
7 Huntzicker, 1995].

8 In Australia, there have been a number of studies aimed at improving our understanding of  
9 ozone chemistry in the cleaner southern hemisphere atmosphere [Galbally *et al.*, 2000;  
10 Monks *et al.*, 1998]; secondary aerosol formation [Caine *et al.*, 2007] or other air quality  
11 issues, such as air toxics and smoke [Hinwood *et al.*, 2007; Keywood *et al.*, 2015]. There have  
12 also been some air quality studies specifically aimed at testing the Australian Air Quality  
13 Forecasting System [Cope *et al.*, 2004] in Sydney [Hess *et al.*, 2004] and Melbourne [Tory *et al.*,  
14 2004]. The primary focus of these studies was testing the prediction of ozone levels in the  
15 urban environment [Cope *et al.*, 2005]. More recent studies have examined regional air  
16 quality in Wollongong [Buchholz *et al.*, 2016] and the effect of a major fire event on air  
17 quality in Sydney and Wollongong [Rea *et al.*, 2016]. There have also been Australian  
18 campaigns focused on understanding aerosol formation and composition, in the urban  
19 environment e.g. [Cheung *et al.*, 2011; Cheung *et al.*, 2012]; coastal environments [Caine *et al.*,  
20 2007; Fletcher *et al.*, 2007; Modini *et al.*, 2009] and within eucalypt forests [Ristovski  
21 *et al.*, 2010; Suni *et al.*, 2008]. In addition, there have been some detailed studies to characterise  
22 the concentrations of VOCs in the clean background atmosphere in the Australasian region  
23 [Colomb *et al.*, 2009; Galbally *et al.*, 2007; Lawson *et al.*, 2015].

24 In this overview paper, we describe a measurement campaign in the small Australian coastal  
25 city of Wollongong, of approximately 292,000 residents. The Wollongong region is bounded  
26 by ocean to the east and by a steep escarpment, covered in eucalypt forest, to the west. The  
27 coastal plain is roughly triangular in shape, being very narrow in the north where the  
28 escarpment meets the sea, and roughly 20 kilometres wide in the south. The region spans  
29 about 50 kilometres of coastline.

30 The MUMBA campaign involved collaboration between three Australian research groups  
31 (the University of Wollongong; the Commonwealth Scientific and Industrial Research  
32 Organisation (CSIRO), and the Australian Nuclear Science and Technology Organisation

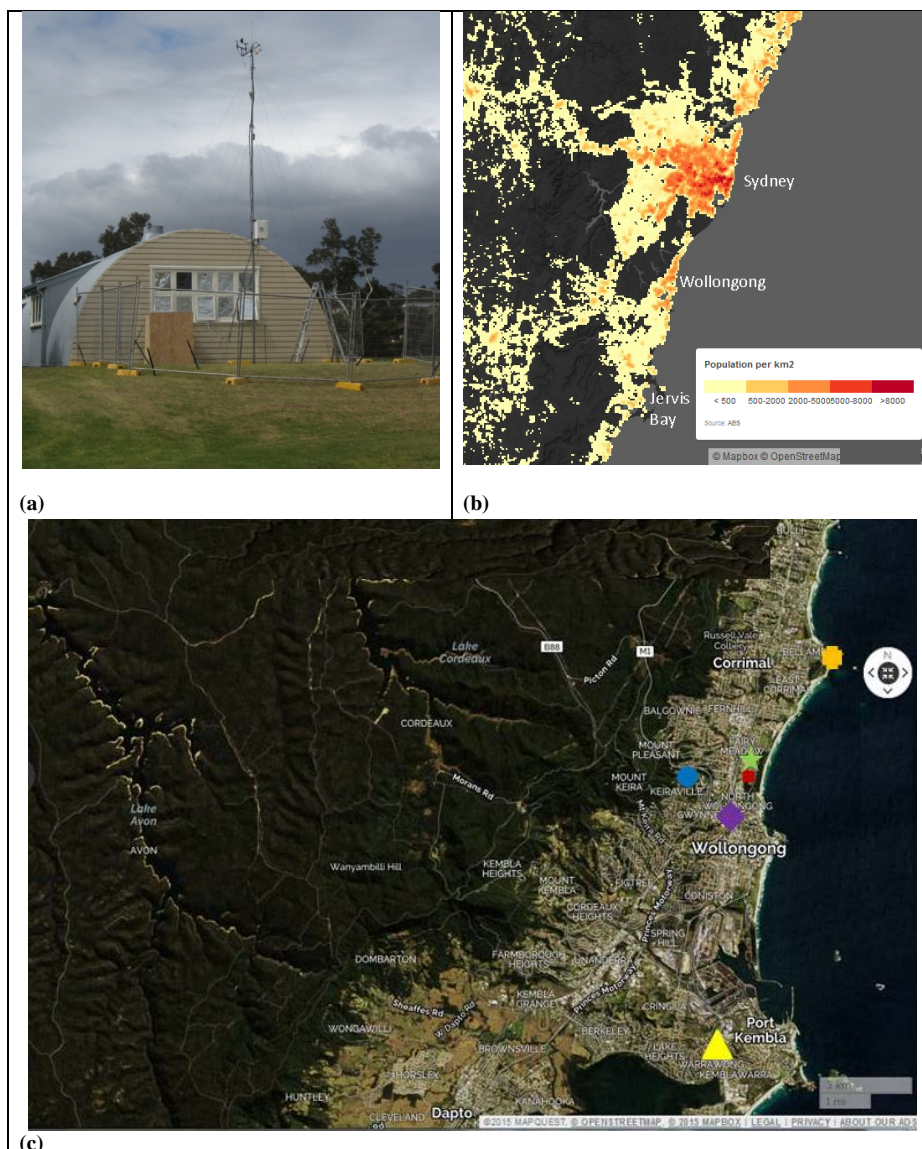


1 (ANSTO), and one research organisation from New Zealand (GNS Science). MUMBA was  
2 designed to provide a comprehensive characterisation of the local atmosphere that could test  
3 the capabilities of air quality models to forecast atmospheric composition. Influences from  
4 the nearby ocean sources, urban emissions and the biogenic emissions from the surrounding  
5 eucalypt forests were expected to impact the site. This campaign aimed to make detailed  
6 measurements of atmospheric composition under the combined influence of these different  
7 sources, all of which typically affect the populated regions of the East coast of Australia.

## 8 **2. Measurement Sites**

9 The MUMBA campaign included instruments that were run at several different, nearby sites.  
10 The main measurement site (34.397°S, 150.900°E) of the MUMBA campaign was located in  
11 a suburban area of Wollongong approximately half a kilometre from the ocean. The  
12 instruments were located in and adjacent to an unused hut located at the University of  
13 Wollongong's campus east (see Figure 1a). Most instruments sampled from a mast at a height  
14 of ~10 m above the surrounding ground level (also shown in Figure 1a). Immediately  
15 surrounding the measurement site is a grassy plain with a suburban road to the east and a strip  
16 of forested parkland beyond, before the sand dunes and ocean. Prevailing easterly sea breezes  
17 brought air-masses from the ocean to the site during the day. Urban influences from the local  
18 metropolitan area and a large industrial area, including a steelworks, typically occurred in  
19 still conditions or with southerly winds. The steep forested escarpment is about 3 km directly  
20 to the west of the site and approximately 400 m high, with the area beyond dominated by  
21 eucalypt forest, such that westerly winds brought strong biogenic signals. The population  
22 density within the surrounding area of New South Wales (NSW), including Wollongong and  
23 Sydney is shown in Figure 1b.

24 The locations of different measurement sites are shown in Figure 1c.



1  
2 **Figure 1:** (a) Hut that hosted most of the instruments during MUMBA and the sample mast. (b) Population  
3 density map for the region based on Australian Bureau of Statistics data from August 2011 –  
4 <http://www.abs.gov.au/AUSSTATS/abs@.nsf/Lookup/1270.0.55.007Main+Features12011?OpenDocument>  
5 (c) Satellite view of the region showing the main MUMBA site (green star), the Wollongong Science Centre  
6 (red square), Wollongong EPA Air Quality station (purple diamond), the University of Wollongong (blue circle),  
7 Bellambi Automatic Weather Station (orange hexagon) and the ANSTO radon detector site at  
8 Warrawong (yellow triangle). The large red square indicates the approximate location of the CHIMERE  
9 grid-space used to compare to the MUMBA observations. Also visible is the large industrial area at Port  
10 Kembla and the extensive forested regions to the West. The image was created using website:  
11 [www.mapquest.com](http://www.mapquest.com) “© OpenStreetMap contributors”.

12



1 In addition, ANSTO provided measurements of atmospheric radon concentrations from  
2 Warrawong (34.48°S, 150.89°E), an industrial suburban site located approximately 10 km to  
3 the south of the main MUMBA site. The use of radon to characterise boundary layer mixing  
4 [*Chambers et al.*, 2011] is likely to be especially useful for testing air quality models, due to  
5 the challenges of modelling within the complex topography of coastal areas. The locations of  
6 all of the sites used in the MUMBA campaign are marked on the satellite view of the region  
7 shown in Figure 1c.

8

### 9 **3. Description of the Instruments Deployed at the Main Measurement** 10 **Site**

11 A large range of instrumentation was deployed to enable a detailed characterisation of  
12 atmospheric composition during the campaign. All measurements made during the campaign  
13 are listed in Table 1. As not all instruments operated for the entire campaign, the dates of  
14 operation of each instrument are given. All data are available from PANGAEA  
15 (<https://doi.pangaea.de/10.1594/PANGAEA.871982>) as hourly averages unless otherwise  
16 specified. Further details of the instruments are given in the Appendix, along with a second  
17 table that lists the specific VOCs measured during the campaign and their limits of detection.  
18 Also available from PANGAEA are the radon measurements made at Warrawong by ANSTO  
19 and the air quality data from the Wollongong Office of Environment and Heritage (OEH)  
20 station. The FTIR spectrometer uses a drier on the inlet and measured mole fraction in dry  
21 air; other gas phase instruments measured in ambient air. All times are reported in local  
22 standard time (UTC +10).

### 23 **4. Additional Measurements**

24 Measurements were also available from the OEH air quality station at Wollongong  
25 (34.419°S, 150.886°E). Additional instruments were operated nearby at the University of  
26 Wollongong's main campus (at 34.406°S, 150.897°E) [*Buchholz et al.*, 2016] and at the  
27 nearby Science Centre (34.401°S, 150.900°E), but the observations are not included here.  
28 Data from the University of Wollongong include retrievals of total column amounts of trace  
29 gases from the Total Carbon Column Observing Network (see <http://www.tccon.caltech.edu/>)  
30 and the Network for Detection of Atmospheric Composition Change (see  
31 <http://www.ndsc.ncep.noaa.gov/>) and in situ greenhouse gas measurements (see  
32 <http://doi.pangaea.de/10.1594/PANGAEA.848263>). The instrument installed at the Science



- 1 Centre was a Multi-Axis Differential Optical Absorption Spectrometer, and the data is
- 2 available from the authors upon request. The Australian Bureau of Meteorology operates an
- 3 Automatic Weather Station (AWS) at Bellambi (34.37°S, 150.93°E). Again, the data are not
- 4 included here but can be requested from the Bureau if needed.





1 **Table 1: Measurements made during the MUMBA campaign, tabulated alongside the time resolution, the instrument type, and the dates the instrument was**  
 2 **operational. Instruments which ran for the full 8 weeks of the MUMBA campaign are shaded in dark grey, aerosol instruments that ran for the second half of the**  
 3 **campaign are shaded in light grey and instruments that ran for a shorter time period have a white background.**

Measured Parameter(s)	Instrument/Technique	Measurement Time Resolution	Reported Time Resolution	Reported units	Measurement Period
O <sub>3</sub>	UV (Thermo 49i)	1 min	1 hr	ppb	Dec 21 <sup>st</sup> – Feb 15 <sup>th</sup>
NO	Chemiluminescence, (Thermo 42i)	1 min	1 hr	ppb	Dec 21 <sup>st</sup> – Feb 15 <sup>th</sup>
NO <sub>2</sub> +	molybdenum converter				
VOCs	PTR-MS (Ionicon)	~3 min	1 hr	ppb	Dec 21 <sup>st</sup> – Feb 15 <sup>th</sup>
CO <sub>2</sub>	FTIR in situ analyser	~3 min	1 hr	ppm	Dec 21 <sup>st</sup> – Feb 15 <sup>th</sup>
CO, CH <sub>4</sub> , N <sub>2</sub> O del <sup>13</sup> C in CO <sub>2</sub>				ppb	
Boundary layer height	Elastic backscatter at 355nm - LIDAR (Leosphere ALS-400)	30 s	20 minutes	metres above ground level	Dec 21 <sup>st</sup> – Feb 15 <sup>th</sup>
wind speed	Campbell Scientific	1 min	1 hr	m/s	Dec 21 <sup>st</sup> – Jan 25 <sup>th</sup>
wind direction	EasyWeather	5 min	1 hr	degrees	Jan 25 <sup>th</sup> – Feb 15 <sup>th</sup>
temperature				degree Celsius	
pressure				mbar	
relative humidity				%	
Total number concentration of condensation nuclei >3nm	Ultrafine Condensation Particle Counter (TSI 3776)	1 s	1 hr	particles/cm <sup>3</sup>	Jan 16 <sup>th</sup> – Feb 15 <sup>th</sup>
Total number concentration of cloud condensation nuclei	Cloud Condensation Nuclei Counter (Droplet Measurement Technologies)	1 s	1 hr	particles/cm <sup>3</sup>	Jan 16 <sup>th</sup> – Feb 15 <sup>th</sup>
Particle number size distribution (~14 nm to ~660 nm)	Scanning mobility particle sizer	~ 5 min	1 hr	diameter: nm particle concentration: dN/dLogDp particles/cm <sup>3</sup>	Jan 16 <sup>th</sup> – Feb 15 <sup>th</sup>
Elemental and organic carbon in PM <sub>2.5</sub> fraction	HiVol sampling – chemical analysis	04:00-09:00 and 10:00-18:00 daily	04:00-09:00 and 10:00-18:00 daily	and ug C/m <sup>3</sup>	Jan 16 <sup>th</sup> – Feb 15 <sup>th</sup>
PM <sub>10</sub> and PM <sub>2.5</sub> elemental	Streaker sampler (PIXE) – ion beam analysis	1 hr	1 hr	ng/m <sup>3</sup>	Jan 21 <sup>st</sup> – Feb 15 <sup>th</sup>





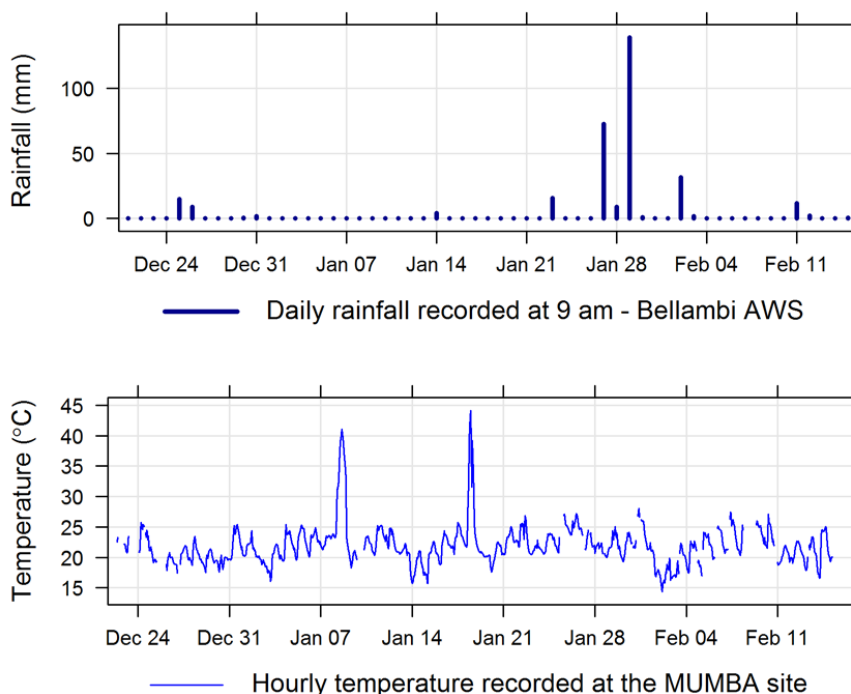
composition					
PM <sub>2.5</sub> mass concentration	Laser scattering (Met One eSampler)	5 min	1 hr	ug/m <sup>3</sup>	Jan 24 <sup>th</sup> – Feb 15 <sup>th</sup>
NO, NO <sub>2</sub>	Chemiluminescence, blue light converter	1 min	1 hr	ppb	Feb 1 <sup>st</sup> – Feb 15 <sup>th</sup>
carbonyls and ketones	2,4-DNPH cartridges/high performance liquid chromatography	04:00-09:00, 10:00-18:00 and 18:00 -04:00 daily	04:00-09:00, 10:00-18:00 and 18:00 -04:00 daily	ppb	Feb 4 <sup>th</sup> – Feb 15 <sup>th</sup>



1        **5. Meteorology during the MUMBA Campaign**

2        The summer of 2012 - 2013 was the hottest summer on record for Australia at the time  
 3        [*White and Fox-Hughes, 2013*]. There were two extremely hot days in the Wollongong region  
 4        during MUMBA, with maximum temperatures of 40.4 °C on January 8<sup>th</sup> and 42.4°C on  
 5        January 18<sup>th</sup> 2013 recorded at Bellambi AWS (both below the record of 43.7°C set on  
 6        January 1<sup>st</sup>, 2006). The campaign encompassed the wettest January day on record for the  
 7        region, with 139 mm of rain falling at Bellambi AWS between 08:00 on January 28<sup>th</sup> and  
 8        08:00 on January 29<sup>th</sup> 2013 (see the top panel of Figure 2).

9        The lower panel of Figure 2 shows the mean hourly temperature recorded from the 10 m mast  
 10        at the MUMBA site over the campaign. The two extremely hot days can be clearly seen in  
 11        this figure. The mean daily maximum temperatures during January 2013 was 25.7°C, which  
 12        is 0.9°C above the long-term average of 24.8°C and in the 95<sup>th</sup> percentile of monthly mean  
 13        maximum temperatures for January at Bellambi AWS (using data from 1988 to the present  
 14        day).

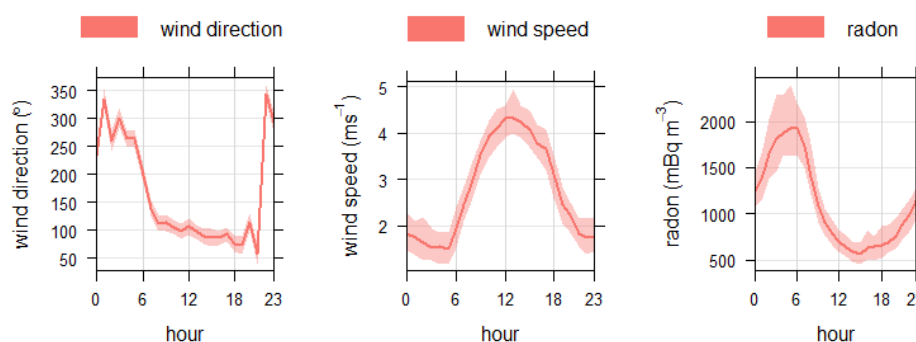


15

16        **Figure 2: Upper panel shows a bar chart of daily rainfall in millimeters from Bellambi AWS. Lower**  
 17        **panel shows the time-series of mean hourly temperature measured during MUMBA.**



1 The average wind speed recorded at the MUMBA site during the campaign was  $2.8 \text{ ms}^{-1}$ , and  
 2 the maximum hourly-averaged wind speed recorded was  $9.2 \text{ ms}^{-1}$ . The 1<sup>st</sup>, 2<sup>nd</sup> (median) and  
 3 3<sup>rd</sup> quartiles of the wind speed were  $1.4 \text{ ms}^{-1}$ ,  $2.6 \text{ ms}^{-1}$  and  $3.9 \text{ ms}^{-1}$  respectively. Figure 3  
 4 shows the composite diel cycles of wind speed and wind direction as measured at the main  
 5 MUMBA site. The general pattern was of a relatively strong sea breeze during the day  
 6 (~easterly winds of  $3\text{--}4 \text{ ms}^{-1}$ ) and of calmer conditions overnight. Westerly winds were more  
 7 frequent during night time (although north-easterly winds sometimes persisted into the night).  
 8 This pattern was repeated all over the local region (as shown in data from OEH air quality  
 9 sites and from the University of Wollongong) [Guérette, 2016].



10

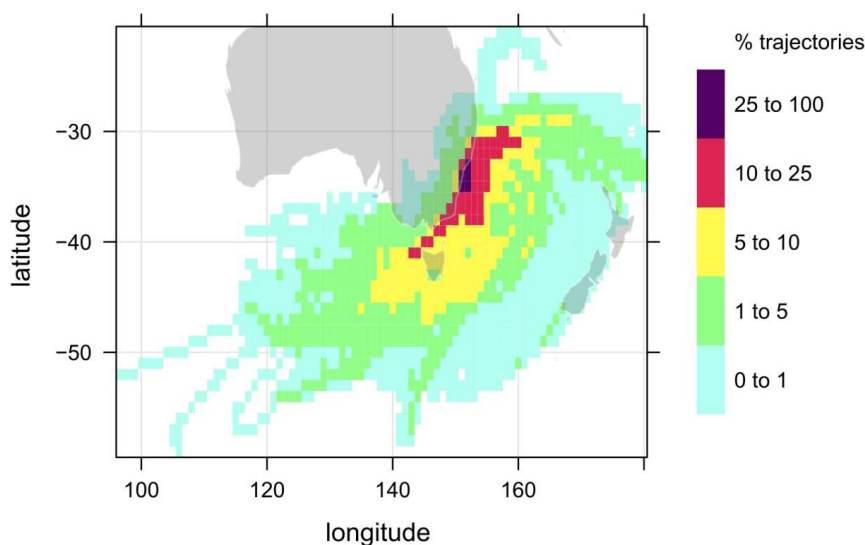
11 **Figure 3: Observed diurnal cycles of wind direction and wind speed at the main MUMBA site and radon**  
 12 **concentration at Warrawang observed during the campaign. (Shaded area shows 95% confidence**  
 13 **interval from a bootstrap resampling of the data. See [Carslaw and Ropkins, 2012] for description of this**  
 14 **and of calculations of average wind direction).**

15 The third panel in Figure 3 shows the composite diel cycle of radon measured at the ANSTO  
 16 site in Warrawang. The radon plot shows a build up at night with a peak in the early hours of  
 17 the morning, indicating a shallower and more stable boundary layer at night than during the  
 18 day, with the boundary layer at its shallowest around 05:00 or 06:00 AEST. During the day,  
 19 due to heating at the surface and other processes, the boundary layer grows deeper and more  
 20 turbulent; this is reflected in the lower radon values observed during the day. Minimum radon  
 21 levels in the afternoon are also influenced by the fetch of the air reaching the site, with air  
 22 that has travelled over the ocean containing less radon than air that has travelled over land  
 23 [Chambers *et al.*, 2015]. In the Wollongong region, an increased boundary layer height and  
 24 strong sea breezes combine to produce the low radon levels observed in the afternoon.

25 Comparisons of the winds measured at the MUMBA site during the campaign, to  
 26 simultaneous measurements at the three air quality sites operated by the Office of  
 27 Environment and Heritage in the area (at Wollongong, Kembla Grange, and Albion Park),



1 indicated that the wind patterns observed at the MUMBA site were generally representative  
2 of the region as a whole [Guérette, 2016]. Long-term average wind data at 15:00 each day are  
3 publically available from the Bellambi AWS from 1997 – 2010, and this was used for  
4 comparison with the wind data recorded at this time throughout January during the campaign.  
5 The MUMBA site in January 2013 was characterised by slightly less frequent northerly  
6 winds and slightly more frequent westerly winds than expected from the long-term average at  
7 Bellambi, but otherwise wind patterns were very similar in the two records. The MUMBA  
8 site experienced lower wind speeds than the long-term averages at Bellambi (but this may be  
9 due to location differences rather than atypical weather patterns) [Guérette, 2016]. Thus we  
10 conclude that the measurements made at the MUMBA site during the campaign should be  
11 broadly representative of the region, as well as of the summer season.



12  
13 **Figure 4: 96 hour gridded back trajectory frequencies during MUMBA. The surface is coloured by the**  
14 **percentage of total trajectories which pass through each grid-box.**  
15

16  
17 On a larger scale, the dominant circulation pattern during MUMBA was anti-cyclonic, with  
18 the main fetch being principally oceanic (as opposed to continental), which is typical of  
19 summer [Chambers *et al.*, 2011]. This is illustrated in Figure 4, which shows a gridded back  
20 trajectory frequency plot for 96-hour pre-calculated back trajectories made available for  
21 Wollongong through the Openair package [Carslaw and Ropkins, 2012]. The trajectories  
22 were calculated using the HYSPLIT trajectory model (Hybrid Single Particle Lagrangian  
23 Integrated Trajectory Model; <http://ready.arl.noaa.gov/HYSPLIT.php>) every three hours,



1 from an initial height of 10 metres and propagated backwards in time for 96 hours using the  
2 Global NOAA-NCEP/NCAR reanalysis meteorological fields at 2.5° horizontal resolution.  
3 The surface of the plot is coloured by the percentage of total trajectories which pass through  
4 each grid-box.

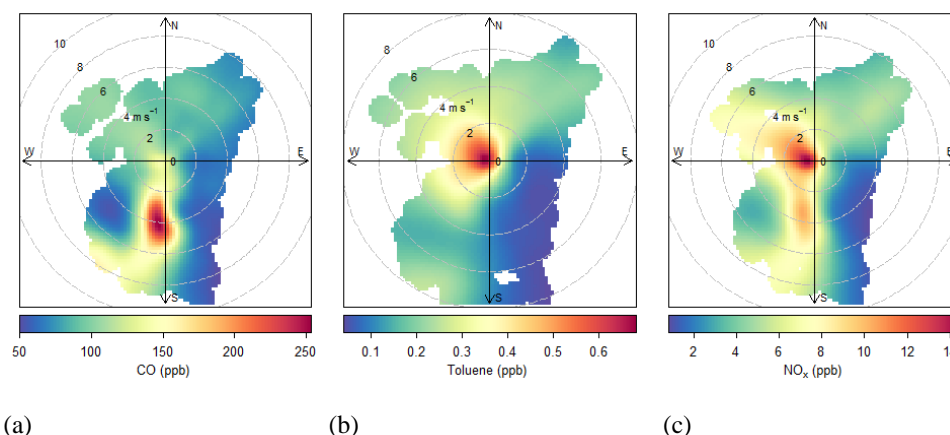
## 5 **6. Urban, Marine and Biogenic Influences during the MUMBA Campaign**

6 The MUMBA campaign was designed to characterise atmospheric composition at the  
7 ocean/forest/urban interface and thereby provide a dataset that could be used to test the skill  
8 of atmospheric models within a coastal environment. In this section, the major urban, marine  
9 and biogenic sources that influence atmospheric composition in the region are described.

10 The dominant anthropogenic sources in the region are the Port Kembla steelworks, located  
11 approximately 10 km south of the main MUMBA site (for PM<sub>2.5</sub>, PM<sub>10</sub>, CO, NO<sub>x</sub> and SO<sub>2</sub>)  
12 and motor vehicles (for NO<sub>x</sub>, CO and VOCs) (see: <http://www.npi.gov.au/npidata>). The  
13 ocean lies to the east of the site and large forested areas to the west. Outflow from the Sydney  
14 basin (80 km to the north) may accompany winds from the north-east.

15 The impact of the different air-masses sampled can be illustrated using a bivariate polar plot,  
16 which shows how a pollutant varies by wind speed and wind direction as suggested by  
17 *Carslaw et al* [2006]. Figure 5a shows a bivariate polar plot for CO measured from the main  
18 MUMBA site throughout the campaign. Several distinct regions are evident, with the most  
19 obvious being the very high amounts of CO that are measured when the site experiences  
20 southerly winds with speeds between 2 and 6 ms<sup>-1</sup>. This direction brings air-masses over  
21 central Wollongong and also over the industrial area centred on the steelworks at Port  
22 Kembla. In contrast, easterly to south-south-easterly winds bring very low amounts of CO to  
23 the MUMBA site as the air-masses come from the Pacific Ocean. There were a number of  
24 occasions during the campaign when easterly winds brought predominantly marine air to the  
25 measurement site. These periods were identified by using radon values below a threshold of  
26 200 mBq m<sup>-3</sup>, indicating minimal terrestrial impact in agreement with back trajectories. One  
27 episode in particular, on December 26<sup>th</sup>, 2012, lasted several hours and was characterised by  
28 greenhouse gas concentrations similar to those measured in December 2012 at the Cape Grim  
29 baseline air pollution station on the north west tip of Tasmania, Australia (40.683°S, 144.689°  
30 E) (see <http://www.csiro.au/greenhouse-gases/>). These episodes are explored further in a  
31 paper dedicated to the marine air signature during MUMBA [*Guérette et al.*, 2017].

32



1 **Figure 5: Bivariate polar plots showing how mole fractions (ppb) of (a) CO, (b) toluene and (c) NO<sub>x</sub> vary**  
2 **as a function of wind speed (ms<sup>-1</sup>) and wind direction at the main MUMBA site during the campaign.**  
3 **Wind speed is represented by the concentric circles and wind direction is shown as compass directions,**  
4 **such that the shape of the coloured area illustrates the wind speeds and directions experienced during the**  
5 **campaign. The colour indicates mean mole fraction measured under the corresponding wind conditions.**  
6

7 CO mole fractions from the north-east (that also come off the ocean) are nearly double those  
8 from the south-south-east, indicating that the MUMBA site may be influenced by outflow  
9 from the Sydney basin, 80 km to the north. Elevated CO is also measured from the north-west  
10 in the direction of the nearest suburban shopping centre, multilane road and local industrial  
11 sites (including a coke-works and mining operations). In contrast, relatively low  
12 concentrations are seen from the south-west where there is a steep escarpment and eucalypt  
13 forests beyond.

14 Figure 5b shows the polar bivariate plot for toluene, which is predominantly emitted from  
15 motor vehicles and is not emitted from the steelworks. The plot shows the largest  
16 concentrations with low wind speeds, as is indicative of local sources building up in the  
17 nocturnal boundary layer, however there is a directional bias with much cleaner air to the  
18 east. This is due to clean marine air coming from the east and is also obvious in the low  
19 amounts of toluene coming from all wind speeds from the south-east. In contrast, there are  
20 slightly higher mole fractions of toluene that accompany winds from the north-east, again  
21 indicating possible outflow from Sydney or more local pollution to the north that is brought  
22 in on the sea breeze.

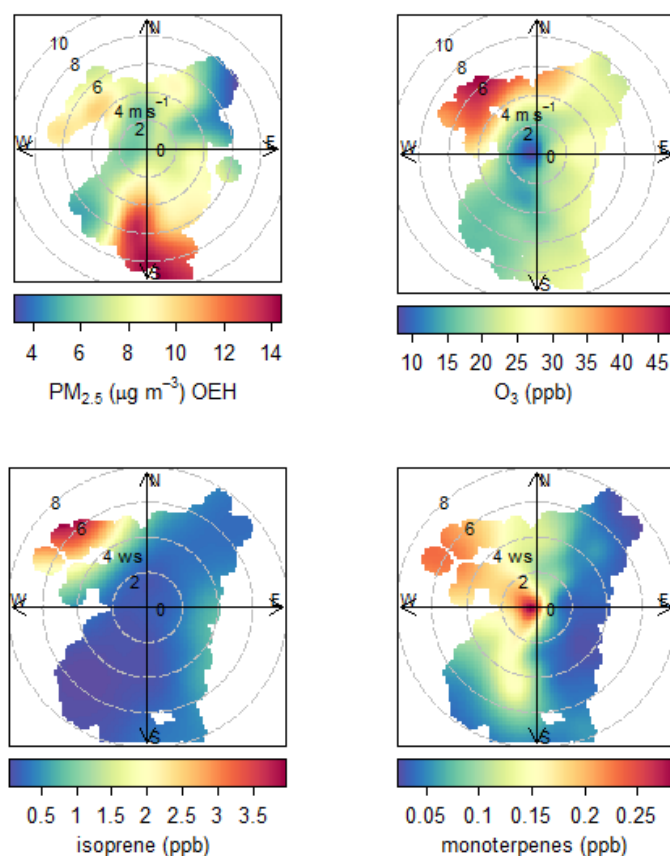
23 Figure 5c shows the polar bivariate plot for NO<sub>x</sub>, which shows a mixture of the features seen  
24 in the toluene and CO plots, indicative of a mixture of traffic and industrial sources as  
25 expected.



1 In Figure 6 polar bivariate plots are shown for the main criteria pollutants of concern within  
2 the air-shed ( $PM_{2.5}$  and  $O_3$ ), along with the most significant biogenic volatile organic  
3 compounds, isoprene (PTR-MS  $m/z$  69) and monoterpenes (PTR-MS  $m/z$  137). Both  
4 isoprene and monoterpenes show very elevated concentrations with strong north-westerlies,  
5 which occurred on the two extremely hot days (January 8<sup>th</sup> and January 18<sup>th</sup> 2013). The  
6 monoterpenes are also high with still winds, because (unlike isoprene) these compounds are  
7 also emitted during the night and hence build up in the nocturnal boundary layer. Also, under  
8 more stable night-time conditions, katabatic flow down the escarpment will bring air  
9 predominantly influenced by the eucalypt forests to the site.

10 The highest  $PM_{2.5}$  concentrations are seen with strong to moderate winds from the south,  
11 which bring industrial sources from the Port Kembla steelworks. Elevated  $PM_{2.5}$  is also seen  
12 with north-westerly winds that bring biogenic influences from the escarpment and densely  
13 forested regions beyond. Highest  $O_3$  concentrations are also seen with the hot north-westerly  
14 winds, with the influence of  $NO_x$  titrating out the  $O_3$  clearly seen with low concentrations  
15 observed at low wind speeds and with wind from the south. The high  $O_3$  and  $PM_{2.5}$  values  
16 that accompany the high levels of isoprene and monoterpenes, imply that biogenic influences  
17 are important for both  $O_3$  formation and secondary organic aerosol formation in the region.  
18 This may be due to having a VOC-limited environment (the formaldehyde to  $NO_x$  ratio  
19 averaged 0.3 over the campaign), coupled to the fact that anthropogenic emissions of VOCs  
20 are relatively low in the area, so that biogenic VOCs are extremely important to the overall  
21 budget. Despite the importance to air quality, biogenic emissions from Australian eucalypt  
22 forests are poorly understood [Emmerson *et al.*, 2016] and further research is needed to better  
23 characterise biogenic emissions in this region of Australia.





1

2 **Figure 6: Bivariate polar plots showing how (a) the concentration of PM<sub>2.5</sub> (μg m<sup>-3</sup>) at the OEH station and**  
3 **mole fractions (ppb) of (b) O<sub>3</sub>, (c) isoprene and (d) monoterpenes at the main MUMBA site, varied as a**  
4 **function of wind speed (ms<sup>-1</sup>) and wind direction during the campaign.**

5

## 6 **7. Summary and Conclusions**

7

8 The combined datasets from MUMBA provide a useful case study for testing the skill of air  
9 quality models in the complex environment of urban, marine and forest influences that exists  
10 in coastal Australia, where the majority of its inhabitants live. This overview paper aims to  
11 provide the reader with sufficient understanding of the MUMBA campaign to use the datasets  
12 as a test case for any air quality model, including an understanding of the Wollongong urban  
13 air-shed, regional topography, emissions and meteorology.



1 During the eight week campaign the MUMBA site experienced some very different  
2 conditions, ranging from relatively polluted air (with local urban pollution from traffic and  
3 nearby industrial sources), to unpolluted marine air with composition akin to that  
4 representative of the remote marine boundary layer measured at the Cape Grim station under  
5 baseline conditions. There were two extreme heat events during MUMBA when westerly  
6 winds brought strong biogenic influences from nearby forested regions. The measurements of  
7 atmospheric composition during these events provide data that could prove to be a valuable  
8 test of models of future air quality in a changing climate.

9 A series of papers are in preparation that describe the main scientific findings from the  
10 MUMBA campaign, including articles focusing on: (1) drivers of urban air quality; (2)  
11 marine air at 34°S; (3) biogenic emissions of volatile organic compounds; (4) drivers of  
12 aerosol loading in the airshed and (5) new particle formation events. In addition, the  
13 MUMBA campaign measurements are being used in conjunction with long-term  
14 measurements from the OEH air quality network, and campaign data from the Sydney  
15 Particle Study campaigns [Keywood *et al.*, 2016a; Keywood *et al.*, 2016b] as observational  
16 datasets in a modelling inter-comparison exercise involving four different regional air quality  
17 models. The MUMBA data is available from PANGAEA  
18 (<https://doi.pangaea.de/10.1594/PANGAEA.871982>) for other researchers wanting to join the  
19 inter-comparison exercise or use the data independently to test atmospheric composition  
20 simulations in the region.

21

22

23

#### 24 **Acknowledgements**

25 The authors would like to thank all those from the University of Wollongong's Centre for  
26 Atmospheric Chemistry and CSIRO's Climate Science Centre group, who helped with the  
27 logistics of undertaking an extensive measurement campaign, and in particular Travis Naylor,  
28 Graham Kettlewell, Christopher Caldw, Frances Phillips, Jason Ward, James Harnwell and  
29 Jenny Fisher. The ANSTO technical staff responsible for installing and maintaining the  
30 Warramong radon detector were Ot Sisoutham and Sylvester Werczynski. Thanks are also  
31 due to Kids Uni & the Science Centre for their helpful support, and to David Carslaw (& all  
32 the statisticians who developed the relevant 'R' code) for public access to the excellent



1 Openair package for analysis of air quality data. We acknowledge funding from the  
2 Australian Research Council (for funding the campaign as part of the Discovery Project  
3 DP110101948) and the Clean Air and Urban Landscapes hub of Australia's National  
4 Environmental Science Programme (for funding for later analysis of results that was required  
5 for producing this manuscript). This research was also supported by Australian Government  
6 Research Training Program (RTP) Scholarships.

7

## 8 References

- 9 Buchholz, R. R., et al. (2016), Source and meteorological influences on air quality (CO, CH<sub>4</sub>  
10 & CO<sub>2</sub>) at a Southern Hemisphere urban site, *Atmospheric Environment*, 126, 274-289,  
11 doi:<http://dx.doi.org/10.1016/j.atmosenv.2015.11.041>.
- 12 Caine, J. M., et al. (2007), Precursors to Particles (P2P) at Cape Grim 2006: campaign  
13 overview, *Environmental Chemistry*, 4(3), 143-150, doi:10.1071/en07041.
- 14 Carslaw, D. C., S. D. Beevers, K. Ropkins, and M. C. Bell (2006), Detecting and quantifying  
15 aircraft and other on-airport contributions to ambient nitrogen oxides in the vicinity of a  
16 large international airport, *Atmospheric Environment*, 40(28), 5424-5434,  
17 doi:10.1016/j.atmosenv.2006.04.062.
- 18 Carslaw, D. C., and K. Ropkins (2012), Openair - An r package for air quality data analysis,  
19 *Environmental Modelling and Software*, 27-28, 52-61,  
20 doi:10.1016/j.envsoft.2011.09.008.
- 21 Castro, L. M., C. A. Pio, R. M. Harrison, and D. J. T. Smith (1999), Carbonaceous aerosol in  
22 urban and rural European atmospheres: estimation of secondary organic carbon  
23 concentrations, *Atmospheric Environment*, 33(17), 2771-2781, doi:10.1016/s1352-  
24 2310(98)00331-8.
- 25 Chambers, S., A. G. Williams, J. Crawford, and A. D. Griffiths (2015), On the use of radon  
26 for quantifying the effects of atmospheric stability on urban emissions, *Atmospheric  
27 Chemistry and Physics*, 15(3), 1175-1190, doi:10.5194/acp-15-1175-2015.
- 28 Chambers, S., A. G. Williams, W. Zahorowski, A. Griffiths, and J. Crawford (2011),  
29 Separating remote fetch and local mixing influences on vertical radon measurements in  
30 the lower atmosphere, *Tellus B*, 63(5), 843-859, doi:10.1111/j.1600-  
31 0889.2011.00565.x.
- 32 Cheng, M., I. E. Galbally, S. B. Molloy, P. W. Selleck, M. D. Keywood, S. J. Lawson, J. C.  
33 Powell, R. W. Gillett and E. Dunne (2015), Factors controlling volatile organic  
34 compounds in dwellings in Melbourne, Australia., *Indoor Air*, doi:10.1111/ina.12201.
- 35 Cheung, H. C., L. Morawska, and Z. D. Ristovski (2011), Observation of new particle  
36 formation in subtropical urban environment, *Atmospheric Chemistry and Physics*,  
37 11(8), 3823-3833, doi:10.5194/acp-11-3823-2011.
- 38 Cheung, H. C., L. Morawska, Z. D. Ristovski, and D. Wainwright (2012), Influence of  
39 medium range transport of particles from nucleation burst on particle number  
40 concentration within the urban airshed, *Atmospheric Chemistry and Physics*, 12(11),  
41 4951-4962, doi:10.5194/acp-12-4951-2012.
- 42 Colomb, A., V. Gros, S. Alvain, R. Sarda-Esteve, B. Bonsang, C. Moulin, T. Klupfel, and J.  
43 Williams (2009), Variation of atmospheric volatile organic compounds over the



- 1 Southern Indian Ocean (30-49 degrees S), *Environ. Chem.*, 6(1), 70-82,  
2 doi:10.1071/en08072.
- 3 Cope, M. E., et al. (2004), The Australian Air Quality Forecasting System. Part I: Project  
4 description and early outcomes, *J. Appl. Meteorol.*, 43(5), 649-662,  
5 doi:10.1175/2093.1.
- 6 Cope, M. E., G. D. Hess, S. Lee, K. J. Tory, M. Burgers, P. Dewundege, and M. Johnson  
7 (2005), The Australian Air Quality Forecasting System: Exploring first steps towards  
8 determining the limits of predictability for short-term ozone forecasting, *Boundary-  
9 Layer Meteorology*, 116(2), 363-384, doi:10.1007/s10546-004-2816-2.
- 10 Dunne, E., I. E. Galbally, M. Cheng, P. Selleck, S. B. Molloy, and S. J. Lawson (2017),  
11 Comparison of VOC measurements made by PTR-MS, Adsorbent Tube/GC-FID-MS  
12 and DNP-derivatization/HPLC during the Sydney Particle Study, 2012: a contribution  
13 to the assessment of uncertainty in current atmospheric VOC measurements, *Atmos.  
14 Meas. Tech. Discuss.*, 2017, 1-24, doi:10.5194/amt-2016-349.
- 15 Emmerson, K. M., et al. (2016), Current estimates of biogenic emissions from eucalypts  
16 uncertain for southeast Australia, *Atmospheric Chemistry and Physics*, 16(11), 6997-  
17 7011, doi:10.5194/acp-16-6997-2016.
- 18 Fehsenfeld, F. C., et al. (1990), Intercomparison of NO<sub>2</sub> Measurement Techniques, *J.  
19 Geophys. Res.-Atmos.*, 95(D4), 3579-3597, doi:10.1029/JD095iD04p03579.
- 20 Fletcher, C. A., G. R. Johnson, Z. D. Ristovski, and M. Harvey (2007), Hygroscopic and  
21 volatile properties of marine aerosol observed at Cape Grim during the P2P campaign,  
22 *Environ. Chem.*, 4(3), 162-171, doi:10.1071/en07011.
- 23 Galbally, I. E., S. T. Bentley, and C. P. Meyer (2000), Mid-latitude marine boundary-layer  
24 ozone destruction at visible sunrise observed at Cape Grim, Tasmania, 41 degrees 5,  
25 *Geophysical Research Letters*, 27(23), 3841-3844, doi:10.1029/1999gl010943.
- 26 Galbally, I. E., S. J. Lawson, I. A. Weeks, S. T. Bentley, R. W. Gillett, M. Meyer, and A. H.  
27 Goldstein (2007), Volatile organic compounds in marine air at Cape Grim, Australia,  
28 *Environ. Chem.*, 4(3), 178-182, doi:10.1071/en07024.
- 29 Gray, H. A., G. R. Cass, and J. J. Huntzicker (1986), Characteristics of atmospheric organic  
30 and elemental carbon particle concentrations in Los Angeles, *Environmental Science  
31 and Technology*, 20(6), 580-589.
- 32 Griffith, D. W. T., N. M. Deutscher, C. Caldwell, G. Kettlewell, M. Riggenbach, and S.  
33 Hammer (2012), A Fourier transform infrared trace gas and isotope analyser for  
34 atmospheric applications, *Atmospheric Measurement Techniques*, 5(10), 2481-2498,  
35 doi:10.5194/amt-5-2481-2012.
- 36 Guérette, É.-A. (2016), Measurements of VOC sources and ambient concentrations in  
37 Australia, PhD Thesis, School of Chemistry, University of Wollongong.
- 38 Guérette, É.-A., et al. (2017), Marine influences during the MUMBA campaign, *Atmospheric  
39 Environment (in prep)*.
- 40 Hess, G. D., K. J. Tory, M. E. Cope, S. Lee, K. Puri, P. C. Manins, and M. Young (2004),  
41 The Australian Air Quality Forecasting System. Part II: Case study of a Sydney 7-day  
42 photochemical smog event, *J. Appl. Meteorol.*, 43(5), 663-679, doi:10.1175/2094.1.
- 43 Hinwood, A. L., et al. (2007), Risk factors for increased BTEX exposure in four Australian  
44 cities, *Chemosphere*, 66(3), 533-541, doi:10.1016/j.chemosphere.2006.05.040.
- 45 Husar, R. B., B. Y. H. Liu, and K. T. Whitby (1972), Physical Mechanisms Governing  
46 Dynamics of Los-Angeles Smog aerosol, *Journal of Colloid And Interface Science*,  
47 39(1), 211-224, doi:10.1016/0021-9797(72)90155-5.
- 48 Keywood, M., M. Cope, C. P. M. Meyer, Y. Iinuma, and K. Emmerson (2015), When smoke  
49 comes to town: The impact of biomass burning smoke on air quality, *Atmospheric  
50 Environment*, 121, 13-21, doi:10.1016/j.atmosenv.2015.03.050.



- 1 Keyword, M., et al. (2016a), Sydney Particle Study 1 - Aerosol and gas data collection. v3. ,  
2 edited by CSIRO, doi:<http://doi.org/10.4225/08/57903B83D6A5D>
- 3 Keyword, M., et al. (2016b), Sydney Particle Study 2 - Aerosol and gas data collection. v1. ,  
4 edited by CSIRO, doi:<http://doi.org/10.4225/08/5791B5528BD63>
- 5 Lawson, S. J., P. W. Selleck, I. E. Galbally, M. D. Keywood, M. J. Harvey, C. Lerot, D.  
6 Helmig, and Z. Ristovski (2015), Seasonal in situ observations of glyoxal and  
7 methylglyoxal over the temperate oceans of the Southern Hemisphere, *Atmospheric*  
8 *Chemistry and Physics*, 15(1), 223-240, doi:10.5194/acp-15-223-2015.
- 9 Modini, R. L., Z. D. Ristovski, G. R. Johnson, C. He, N. Surawski, L. Morawska, T. Suni,  
10 and M. Kulmala (2009), New particle formation and growth at a remote, sub-tropical  
11 coastal location, *Atmospheric Chemistry and Physics*, 9(19), 7607-7621,  
12 doi:10.5194/acp-9-7607-2009.
- 13 Monks, P. S., L. J. Carpenter, S. A. Penkett, G. P. Ayers, R. W. Gillett, I. E. Galbally, and C.  
14 P. Meyer (1998), Fundamental ozone photochemistry in the remote marine boundary  
15 layer: The SOAPEX experiment, measurement and theory, *Atmospheric Environment*,  
16 32(21), 3647-3664, doi:10.1016/s1352-2310(98)00084-3.
- 17 Morille, Y., M. Haeffelin, P. Drobinski, and J. Pelon (2007), STRAT: An automated  
18 algorithm to retrieve the vertical structure of the atmosphere from single-channel lidar  
19 data, *Journal of Atmospheric and Oceanic Technology*, 24(5), 761-775,  
20 doi:10.1175/jtech2008.1.
- 21 Rea, G., C. Paton-Walsh, S. Turquety, M. Cope, and D. Griffith (2016), Impact of the New  
22 South Wales fires during October 2013 on regional air quality in eastern Australia,  
23 *Atmos. Environ.*, 131, 150-163, doi:10.1016/j.atmosenv.2016.01.034.
- 24 Ristovski, Z. D., T. Suni, M. Kulmala, M. Boy, N. K. Meyer, J. Duplissy, A. Turnipseed, L.  
25 Morawska, and U. Baltensperger (2010), The role of sulphates and organic vapours in  
26 growth of newly formed particles in a eucalypt forest, *Atmospheric Chemistry and*  
27 *Physics*, 10(6), 2919-2926, doi:10.5194/acp-10-2919-2010.
- 28 Steinbacher, M., C. Zellweger, B. Schwarzenbach, S. Bugmann, B. Buchmann, C. Ordonez,  
29 A. S. H. Prevot, and C. Hueglin (2007), Nitrogen oxide measurements at rural sites in  
30 Switzerland: Bias of conventional measurement techniques, *J. Geophys. Res.-Atmos.*,  
31 112(D11), D11307, doi:10.1029/2006jd007971.
- 32 Suni, T., et al. (2008), Formation and characteristics of ions and charged aerosol particles in a  
33 native Australian Eucalypt forest, *Atmospheric Chemistry and Physics*, 8(1), 129-139,  
34 doi:10.5194/acp-8-129-2008.
- 35 Tory, K. J., M. E. Cope, G. D. Hess, S. Lee, K. Puri, P. C. Manins, and N. Wong (2004), The  
36 Australian Air Quality Forecasting System. Part III: Case study of a Melbourne 4-day  
37 photochemical smog event, *J. Appl. Meteorol.*, 43(5), 680-695, doi:10.1175/2092.1.
- 38 Turpin, B. J., and J. J. Huntzicker (1995), Identification of Secondary Organic Aerosol  
39 Episodes and Quantification of Primary and Secondary Organic Aerosol Concentrations  
40 During SCAQS, *Atmospheric Environment*, 29(23), 3527-3544, doi:10.1016/1352-  
41 2310(94)00276-q.
- 42 Whitby, K. T., R. B. Husar, and B. Y. H. Liu (1972a), The aerosol size distribution of Los  
43 Angeles smog, *Journal of Colloid And Interface Science*, 39(1), 177-204.
- 44 Whitby, K. T., B. Y. H. Liu, R. B. Husar, and N. J. Barsic (1972b), The minnesota aerosol-  
45 analyzing system used in the Los Angeles smog project, *Journal of Colloid And*  
46 *Interface Science*, 39(1), 136-164.
- 47 White, C. J., and P. Fox-Hughes (2013), Seasonal climate summary southern hemisphere  
48 (summer 2012-13): Australia's hottest summer on record and extreme east coast rainfall,  
49 *Australian Meteorological and Oceanographic Journal*, 63, 443-456.
- 50



## 1 **Appendix 1: Details of the Instruments Used**

### 2 **1. PTR-MS**

3 An “IONICON” proton transfer reaction mass spectrometer (PTR-MS) from CSIRO operated  
4 throughout the MUMBA campaign. The PTR-MS was installed along with the auxiliary  
5 equipment that controls the flow rate and incorporates regular sampling of calibration gases  
6 and “zero air” [Galbally *et al.*, 2007]. The instrument performed zero measurements twice  
7 daily for 40 minutes each time (at 00:50 and at 15:00 local time) by sampling ambient air that  
8 had been stripped of volatile organic compounds (VOCs) by passing through a platinum-  
9 coated glass wool catalyst heated to 350°C. A multi-species, single-point calibration was  
10 performed daily (from 01:30 until 03:00 local time) by introducing a known flow of  
11 calibration standard into the zero air stream. Calibration mole fractions were ~10 to 20 ppb  
12 for each VOC present in the standard.

13 The PTR-MS was operated using  $\text{H}_3\text{O}^+$  ions only and was programmed to scan through its  
14 range of mass-to-charge ratios ( $m/z$ ) with a dwell time of one second, for a total cycle time of  
15 about three minutes. Mole fractions of volatile organic compounds were calculated from the  
16 PTR-MS at the following masses: formaldehyde (mass 31), methanol (mass 33), acetonitrile  
17 (mass 42), acetaldehyde (mass 45), acetone (mass 59), isoprene (mass 69); isoprene oxidation  
18 products methacrolein and methyl vinyl ketone (mass 71); benzene (mass 79), toluene (mass  
19 93), xylenes (mass 107), trimethyl benzenes (mass 121) and monoterpenes (mass 137).  
20 Further details of these measurements, calibrations and corrections can be found in Guérette  
21 [2016].

### 22 **2. VOC sequencer**

23 From 4<sup>th</sup> to 15<sup>th</sup> February 2013, continuous VOC measurements made using the PTR-MS  
24 were supplemented by integrated measurements collected on the VOC sequencer. The VOC  
25 sequencer passes air samples through two different adsorbent tubes to collect the VOCs and  
26 the carbonyls respectively. These tubes were analysed at CSIRO on a gas chromatography  
27 flame ionisation detection/mass spectrometer (GC-FID-MS) for VOCs [Cheng, 2015] and  
28 HPLC for carbonyls [Lawson *et al.*, 2015], which enables unambiguous species identification  
29 (which is not always provided by product ion mass numbers from the PTR-MS) at 5, 8 or 10-  
30 hour temporal resolution [Dunne *et al.*, 2017]. Unfortunately, there was a suspected leak on  
31 the VOC tube side, (with very low concentrations measured), such that none of these data  
32 could be used. In addition there were condensation issues for the carbonyl tubes and only a





1 subset of the species could be determined with confidence. A list of the species measured  
2 successfully using the sequencer is given in Table 2.

### 3 **3. Fourier transform Infra-red (FTIR) Trace Gas Analysers**

4 FTIR trace gas analysers measure carbon dioxide (CO<sub>2</sub>), methane (CH<sub>4</sub>), carbon monoxide  
5 (CO) and nitrous oxide (N<sub>2</sub>O) in air with precision and accuracy that meet the World  
6 Meteorological Organisation - Global Atmosphere Watch standards for baseline air. In  
7 addition the instrument can measure and <sup>13</sup>C in CO<sub>2</sub> and retains the spectra allowing post  
8 analysis for other infrared active trace gases in highly polluted episodes [*Griffith et al.*,  
9 2012]. The instrument ran throughout the whole MUMBA campaign, with the only data  
10 interruption due to the cell temperature going above the range calibrated for on the 18<sup>th</sup>  
11 January 2013. In theory the instrument could be retrospectively recalibrated at the higher  
12 temperatures but since all other instruments had been switched off in the heat this was not  
13 attempted. In addition to the instrument at the main MUMBA site, another FTIR trace gas  
14 analyser was operated throughout the campaign at the main campus of the University of  
15 Wollongong [*Buchholz et al.*, 2016].

16

### 17 **4. NO<sub>x</sub> and O<sub>3</sub> Monitors**

18 Throughout the MUMBA campaign O<sub>3</sub> and NO<sub>x</sub> measurements were made using monitors  
19 that utilised UV absorption and chemiluminescence techniques respectively. The NO-NO<sub>2</sub>-  
20 NO<sub>x</sub> monitor (Thermo Scientific Instruments, model TSI 42i,) detects NO using the  
21 chemiluminescence technique. NO<sub>2</sub> is measured via decomposition to NO by passing over a  
22 molybdenum converter. The difference between the NO concentrations in the two samples is  
23 used to calculate the NO<sub>2</sub> concentration. One issue with this technique is that other nitrates  
24 (such as PAN and HNO<sub>3</sub>) may be present and are also converted to NO by molybdenum but  
25 with different unknown efficiencies [*Steinbacher et al.*, 2007]. In order to get an indication of  
26 the likely level of this problem a second NO<sub>x</sub> monitor from CSIRO was deployed in the last  
27 two weeks of the campaign. This NO<sub>x</sub> monitor uses a blue-light converter so that only the  
28 NO<sub>2</sub> is converted photolytically to NO [*Fehsenfeld et al.*, 1990]. The analysers were within  
29 5% of each other for both NO and NO<sub>2</sub>.





## 1        **5. Micro-physical Particle Counters**

2        From 16<sup>th</sup> January to 15<sup>th</sup> February 2013 a suite of microphysical particle counters was  
3        operated at the main MUMBA site taking ambient air through an 8 m copper inlet mounted  
4        on the mast at a height of ~9.5 m above the surrounding flat area.

5        An ultrafine condensation particle counter (uCPC, TSI model 3776) measured the total in-situ  
6        number concentration of condensation nuclei >3 nm. Particles enter a supersaturated butanol  
7        chamber and all particles > 3nm are grown to sizes that were able to be counted with a  
8        standard optical counter.

9        A Cloud Condensation Nuclei Counter (CCNC) made by Droplet Measurement Technologies  
10       was used to measure the total number concentration of Cloud Condensation Nuclei (CCN).  
11       The instrument operates by similar principle as the CPC, where aerosols are passed through a  
12       supersaturated chamber of liquid, except that water is used instead of butanol. Only particles  
13       able to act as CCN are thus activated and counted. The instrument was setup to measure  
14       particles activated at a supersaturation of 0.5%.

15       The particle number size distribution from ~14 nm to ~660 nm was measured with a scanning  
16       mobility particle sizer (SMPS). The SMPS (TSI model 3080 with DMA 3081 and TSI CPC  
17       3772) ionises particles using radiation from Kr-85 decay. The charged particles then enter an  
18       electrostatic column which ramps its voltage to continually select particles based on their  
19       charge-mass ratio. Selected particles are then counted by a standard CPC.

20       Total PM<sub>2.5</sub> aerosol mass concentration measurements were also made using a Met One  
21       eSampler utilising laser scattering techniques (from 24<sup>th</sup> January to 15<sup>th</sup> February). The  
22       aerosol mass concentration is calibrated via the mass of an integrated sample collected on a  
23       filter that was changed weekly.

## 24       **6. Filter Samplers**

25       Filter samples of total PM<sub>2.5</sub> aerosol were collected twice daily using an Ecotech High  
26       Volume Air Sampler (HiVol). Integrated morning samples were collected on filters from  
27       04:00 and 09:00 each day, with integrated afternoon samples from 10:00 to 18:00 each day.  
28       Thus two filter changes were required (one between 09:00 and 10:00 and another after 18:00  
29       and before 04:00). The filters were taken back to CSIRO for aerosol chemical composition  
30       analysis.

31       A small section (~0.5 cm<sup>2</sup>) of each filter was punched out and the total collected PM<sub>2.5</sub>  
32       aerosol analysed for its total carbon content, elemental carbon (EC) and organic carbon (OC)



1 content using a Thermal Optical Carbon Analyser (Model 2001A). The HiVol instrument  
2 logs the total flow of air that has been passed through each filter and so the total carbon, EC  
3 and OC in the integrated sample of air can be calculated in  $\mu\text{g}/\text{m}^3$ .

4 Also deployed was a Streaker Sampler from GNS Science. This sampler slowly rotates a disk  
5 holding two filters taking ~48 hours for a full revolution. The filters were changed every two  
6 days between 09:00 and 10:00. Only a small section of the filter is required for elemental  
7 composition analysis such that hourly measurements of black carbon and all elements from  
8 sodium to uranium on the periodic table are obtained.

## 9 **7. LIDAR**

10 Throughout the MUMBA campaign ANSTO provided a Leosphere ALS-400 cloud and  
11 aerosol LIDAR that measures elastic backscatter at 355 nm, which is proportional to aerosol  
12 density. By plotting the (range-corrected) backscatter against height, a vertical profile of  
13 aerosol density is created. A negative gradient in aerosol density as represented in the vertical  
14 profiles is indicative of a reduction in aerosol density, and therefore a candidate for the  
15 boundary layer height. Boundary layer heights were estimated via two methods:

16 (1) Visually from plots of the logarithm of the range-corrected 355 nm signal against  
17 height

18 (2) Using the “STRAT” algorithm [Morille *et al.*, 2007].

19 Since this technique relies on clear skies and sufficient aerosol loading to provide a strong  
20 backscatter signal, it is not always possible to determine the boundary layer height with  
21 confidence. Both estimates of boundary layer height with 20-minute resolution are included  
22 in the PANGAEA dataset (<https://doi.pangaea.de/10.1594/PANGAEA.871982>).

## 23 **8. Weather Station**

24 Two different weather stations operated during MUMBA providing common meteorological  
25 parameters including temperature, humidity, pressure, wind speed and direction. The switch  
26 occurred on the 25<sup>th</sup> January when the original (borrowed) weather station was needed for  
27 another field campaign. The Digitech system operated at 5-minute resolution and provided  
28 wind direction as 16 quadrants only, whereas the original station (Campbell Scientific Inc.)  
29 operated at 1-minute resolution and provided wind direction with degree resolution. Both  
30 records are available on PANGAEA as hourly averages.

31



## 1 Appendix 2: List of VOCs Measured

Species	formula	MW	Measurement technique	Time Resolution	n	DL (ppb)	n < DL
formaldehyde	C <sub>2</sub> H <sub>4</sub> O	30.03	DNPH-derivatization/HPLC	04:00 – 09:00	12	0.019	
				10:00 – 18:00	11	0.012	0
				18:00 – 04:00	9	0.009	
			PTR-MS m/z 31	hourly	1027	0.205 0.105 0.186	23
methanol	CH <sub>3</sub> OH	32.04	PTR-MS m/z 33	hourly	1027	0.050 0.033 0.062	0
acetonitrile	C <sub>2</sub> H <sub>3</sub> N	41.05	PTR-MS m/z 42	hourly	1027	0.002 0.001 0.002	0
acetaldehyde	C <sub>2</sub> H <sub>4</sub> O	44.05	DNPH-derivatization/HPLC	04:00 – 09:00	12	0.018	
				10:00 – 18:00	11	0.011	1*
				18:00 – 04:00	9	0.009	
			PTR-MS m/z 45	hourly	1027	0.018 0.007 0.012	0
Glyoxal	C <sub>2</sub> H <sub>2</sub> O <sub>2</sub>	58.04	DNPH-derivatization/HPLC	04:00 – 09:00	12	0.011	
				10:00 – 18:00	11	0.007	0
				18:00 – 04:00	9	0.006	
acetone			PTR-MS m/z 59	hourly	1027	0.010 0.013 0.007	0
Propanal	C <sub>3</sub> H <sub>6</sub> O	58.08	DNPH-derivatization/HPLC	04:00 – 09:00	12	0.011	
				10:00 – 18:00	11	0.007	4
				18:00 – 04:00	9	0.006	
isoprene			PTR-MS m/z 69	Hourly	1029	0.003 0.005 0.003	2
sum of methacrolein and methyl vinyl ketone	C <sub>4</sub> H <sub>6</sub> O	70.09	PTR-MS m/z 71	Hourly	1027	0.004 0.005 0.002	0
methylglyoxal	C <sub>3</sub> H <sub>4</sub> O <sub>2</sub>	72.02	DNPH-derivatization/HPLC	04:00 – 09:00	12	0.006	
				10:00 – 18:00	11	0.003	0
				18:00 – 04:00	9	0.003	
benzene			PTR-MS m/z 79**	hourly	1029	0.010 0.012 0.007	14



toluene			PTR-MS m/z 93			1029	0.005 0.008 0.004	1
hexanal	C <sub>6</sub> H <sub>12</sub> O	100.16	DNPH-derivatization/HPLC	04:00 – 09:00	–	12	0.008 ppb	
				10:00 – 18:00	–	11	0.005 ppb	2
				18:00 – 04:00	–	9	0.004 ppb	
benzaldehyde	C <sub>7</sub> H <sub>6</sub> O	106.12	DNPH-derivatization/HPLC	04:00 – 09:00	–	12	0.003	
				10:00 – 18:00	–	11	0.002	1
				18:00 – 04:00	–	9	0.002	
sum of compounds	C <sub>8</sub> H <sub>10</sub>	106.16	PTR-MS m/z 107			1029	0.003 0.016 0.009	13
sum of compounds	C <sub>9</sub> H <sub>12</sub>	120.20	PTR-MS m/z 121	hourly		1029	0.003 0.013 0.006	2
sum of monoterpenes			PTR-MS m/z 137	hourly		1029	0.007 0.016 0.007	29

1 #note that the PTRMS was run under three differing instrumental settings (due to an accidental change in  
 2 dwell time setting). Thus 3 different detection limits are listed. See metadata in PANGAEA for more details.

3 \*An additional 11 data points were excluded due to analytical problems

4